

Submit a Manuscript: <https://www.f6publishing.com>*World J Gastroenterol* 2025 March 21; 31(11): 100785

DOI: 10.3748/wjg.v31.i11.100785

ISSN 1007-9327 (print) ISSN 2219-2840 (online)

ORIGINAL ARTICLE

Basic Study

NAD+/SIRT1 pathway regulates glycolysis to promote oxaliplatin resistance in colorectal cancer

Ya-Ru Niu, Mi-Dan Xiang, Wen-Wei Yang, Yu-Ting Fang, Hai-Li Qian, Yong-Kun Sun

Specialty type: Gastroenterology and hepatology**Ya-Ru Niu, Mi-Dan Xiang, Wen-Wei Yang, Yu-Ting Fang, Yong-Kun Sun**, Department of Medical Oncology, National Cancer Center/National Clinical Research Center for Cancer/Cancer Hospital, Chinese Academy of Medical Sciences and Peking Union Medical College, Beijing 100021, China**Provenance and peer review:**

Unsolicited article; Externally peer reviewed.

Peer-review model: Single blind**Hai-Li Qian**, National Key Laboratory of Molecular Oncology, National Cancer Center/National Clinical Research Center for Cancer/Cancer Hospital, Chinese Academy of Medical Sciences and Peking Union Medical College, Beijing 100021, China**Peer-review report's classification****Scientific Quality:** Grade A, Grade A, Grade B, Grade C**Co-first authors:** Ya-Ru Niu and Mi-Dan Xiang.**Novelty:** Grade A, Grade B, Grade B, Grade B**Corresponding author:** Yong-Kun Sun, PhD, Chief Doctor, Department of Medical Oncology, National Cancer Center/National Clinical Research Center for Cancer/Cancer Hospital, Chinese Academy of Medical Sciences and Peking Union Medical College, No. 17 Panjiayuan Nanli, Chaoyang District, Beijing 100021, China. hsunyk@cicams.ac.cn**Creativity or Innovation:** Grade A, Grade A, Grade B, Grade B

Abstract

Scientific Significance: Grade A, Grade B, Grade B, Grade B

BACKGROUND

P-Reviewer: Han ZG; Jiao Y; Wang RGlycolysis provides growth advantages and leads to drug resistance in colorectal cancer (CRC) cells. SIRT1, an NAD⁺-dependent deacetylase, regulates various cellular processes, and its upregulation results in antitumor effects. This study investigated the role of SIRT1 in metabolic reprogramming and oxaliplatin resistance in CRC cells.**Received:** August 27, 2024

AIM

Revised: December 13, 2024

To investigate the role of SIRT1 in metabolic reprogramming and overcoming oxaliplatin resistance in CRC cells.

Accepted: February 13, 2025

METHODS

Published online: March 21, 2025We performed transcriptome sequencing of human CRC parental cells and oxaliplatin-resistant cells to identify differentially expressed genes. Key regulators were identified via the LINCS database. NAD⁺ levels were measured by flow cytometry, and the effects of SIRT1 on oxaliplatin sensitivity were assessed by MTS assays, colony formation assays, and xenograft models. Glycolytic function was measured using Western blot and Seahorse assays.**Processing time:** 199 Days and 0.9 Hours

RESULTS



Salermide, a SIRT1 inhibitor, was identified as a candidate compound that

enhances oxaliplatin resistance. In oxaliplatin-resistant cells, SIRT1 was downregulated, whereas γH2AX and PARP were upregulated. PARP activation led to NAD⁺ depletion and SIRT1 inhibition, which were reversed by PARP inhibitor treatment. The increase in SIRT1 expression overcame oxaliplatin resistance, and while SIRT1 inhibition increased glycolysis, the increase in SIRT1 inhibited glycolysis in resistant CRC cells, which was characterized by reduced expression of the glycolytic enzymes PKM2 and LDHA, as well as a decreased extracellular acidification rate. The PKM2 inhibitor shikonin inhibited glycolysis and reversed oxaliplatin resistance induced by SIRT1 inhibition.

CONCLUSION

SIRT1 expression is reduced in oxaliplatin-resistant CRC cells due to PARP activation, which in turn increases glycolysis. Restoring SIRT1 expression reverses oxaliplatin resistance in CRC cells, offering a promising therapeutic strategy to overcome drug resistance.

Key Words: Colorectal cancer; Chemotherapy resistance; Glycolysis; SIRT1; NAD⁺

©The Author(s) 2025. Published by Baishideng Publishing Group Inc. All rights reserved.

Core Tip: SIRT1, a NAD⁺-dependent deacetylase, has demonstrated anti-tumor effects in numerous studies. However, the role of SIRT1 in regulating oxaliplatin resistance remains unclear. This study found that *SIRT1* expression is downregulated in oxaliplatin-resistant colorectal cancer (CRC) cell. Enhancing *SIRT1* expression reverses this resistance. Mechanistically, DNA damage-induced PARP activation inhibits SIRT1 expression. The inhibition of SIRT1 promotes drug resistance in CRC cells by enhancing glycolysis. These findings highlight the critical role of SIRT1 in oxaliplatin resistance and support the potential of combining SIRT1 agonists with oxaliplatin as a therapeutic strategy to overcome CRC resistance.

Citation: Niu YR, Xiang MD, Yang WW, Fang YT, Qian HL, Sun YK. NAD⁺/SIRT1 pathway regulates glycolysis to promote oxaliplatin resistance in colorectal cancer. *World J Gastroenterol* 2025; 31(11): 100785

URL: <https://www.wjgnet.com/1007-9327/full/v31/i11/100785.htm>

DOI: <https://dx.doi.org/10.3748/wjg.v31.i11.100785>

INTRODUCTION

Colorectal cancer (CRC) is the third most common cancer globally, with approximately 1.8 million new cases and 0.9 million deaths each year in 2020, while its mortality rate is the second highest worldwide[1]. CRC currently accounts for approximately 10% of all cancers, and there will be 2.5 million new cases globally by 2035. Around 20% of CRC patients already present with metastases at the time of diagnosis, and up to 50% of those initially diagnosed with localized disease will eventually develop metastatic disease[2,3]. Moreover, 20%-25% of patients undergoing curative surgery will experience recurrence, and require adjuvant chemotherapy. Adjuvant chemotherapy aims to reduce the risk of recurrence by eradicating subclinical tumor deposits that may remain after surgery[4]. According to the National Comprehensive Cancer Network guidelines, patients with advanced-stage CRC should undergo comprehensive treatment that includes surgery, chemotherapy, radiotherapy, and interventional therapies. The FOLFOX and CapOx regimens, which are based on oxaliplatin, are the first-line chemotherapy treatment regimens for advanced-stage CRC[5]. Oxaliplatin can prolong the median disease-free survival and overall survival (OS) of patients with advanced-stage CRC. However, clinical data indicate that only approximately 40%-50% of patients with advanced CRC benefit from this treatment[6]. Indeed, targeted therapies combined with traditional chemotherapy can improve response and survival for patients with metastatic CRC. However, the five-year survival rate of patients with advanced disease remains low, ranging from 10% to 30%[7]. Some CRC cells exhibit primary or acquired resistance to oxaliplatin-based chemotherapy regimens, which leads to cancer deterioration and progression[8]. The development of drug resistance is a multifactorial process, with emerging evidence highlighting the significance of genetic and epigenetic factors in mediating chemoresistance[9,10]. For example, the E3 ubiquitin ligase UBR5 can inhibit the proteasomal degradation of Smad3 through Lys 11-linked polyubiquitination, thereby promoting the transcriptional repression of ATF3, inducing the expression of SLC7A11, and inhibiting ferroptosis, resulting in chemoresistance eventually[11]. Additionally, long non-coding RNA ELFN1-AS1 can enhance DNMT3A-mediated hypermethylation of the MEIS1 promoter, leading to its transcriptional repression. This reduction in MEIS1 expression can upregulate the DNA repair gene FEN1, to decrease oxaliplatin sensitivity in CRC cells[12]. However, it is still poorly understood with regard to the precise molecular mechanisms underlying oxaliplatin resistance, highlighting an urgent requirement for further exploration of these mechanisms.

Chemotherapy resistance is typically associated with complex mechanisms, including increased activity of detoxification systems, inhibition of pathways promoting cell death, increased efficiency of DNA damage repair processes, and increased expression of drug efflux pumps[13]. Moreover, growing evidence suggests that glycolysis is also linked to chemotherapy resistance. For instance, a recent study found that lnc-RP11-536 K7.3 promotes glycolysis through the SOX2/USP7/HIF-1α signaling axis, contributing to chemoresistance in CRC[14]. In addition to the factors mentioned

above, understanding the mechanisms underlying the anti-tumor effects of platinum-based drugs is crucial for investigating chemotherapy resistance mechanisms. Platinum-based drugs act on DNA primarily by forming platinum-DNA complexes, thereby inhibiting tumors by inducing intracellular DNA damage[15,16]. DNA damage responses often trigger multiple intracellular pathways. For example, lipopolysaccharides induce rapid and extensive DNA damage in macrophages, along with the activation of PARP, which leads to the depletion of nicotinamide adenine dinucleotide (NAD+)[17]. NAD⁺ is a dinucleotide coenzyme and a crucial metabolite that functions as a cosubstrate for multiple cellular pathways[18]. It plays a crucial role in regulating key processes involved in tumorigenesis, including maintaining genome stability, managing metabolism, and controlling cell growth and death[19].

NAD⁺ serves as a common substrate to modulate the activity of NAD⁺-consuming enzymes, including sirtuins and PARPs[20]. SIRT1 is an NAD⁺-dependent deacetylase that plays a crucial role in the deacetylation of both histone and nonhistone lysine residues, and thus, SIRT1 participates in the regulation of CRC progression, invasion, and treatment response[21]. SIRT1 has been demonstrated to participate in various pathways that regulate cancer, including the promotion of apoptosis, the inhibition of DNA damage and repair, and the induction of autophagy. For example, SIRT1 regulates two known p53-mediated apoptotic pathways (p53 transcription-dependent and p53 transcription-independent)[22]. SIRT1 deacetylates p53 and blocks its nuclear translocation, which leads to the accumulation of p53 in the cytoplasm and mitochondria and ultimately results in transcription-independent p53-induced apoptosis[23]. Numerous studies have shown that SIRT1 overexpression promotes its antitumor effects by regulating tumor cell apoptosis[24], autophagy[25], and DNA damage repair[26] processes. Additionally, many studies have shown that SIRT1 is involved in glucose and lipid metabolism[27] and mitochondrial biogenesis[28]. For example, the inhibition of SIRT1 expression in liver cancer stem cells enhances the acetylation of the mitochondrial ribosomal protein S5, which promotes its nuclear translocation and in turn enhances the expression of glycolytic proteins and the Warburg effect in liver cancer stem cells[29]. However, the role and mechanisms of the NAD⁺/SIRT1 pathway in chemotherapy resistance remain to be fully elucidated.

Under normoxic conditions, normal cells undergo oxidative phosphorylation, where glucose is converted to pyruvate in the cytoplasm, after which pyruvate enters the mitochondria to enter the tricarboxylic acid cycle, which produces adenosine triphosphate (ATP) for energy. Cancer cells prioritize glycolysis for energy production through metabolic reprogramming. In this process, pyruvate is reduced to lactate in the cytoplasm to generate energy, a phenomenon known as the Warburg effect[30,31]. This metabolic reprogramming gives tumor cells a growth advantage and promotes cancer progression[32]. Pyruvate kinase (PK) is the final rate-limiting enzyme in glycolysis and catalyzes the third irreversible reaction[33]. It converts phosphoenolpyruvate to pyruvate and generates ATP in the process. At least four different isoforms of PK have been defined (M1, M2, L, and R), among which PKM2 is the primary isoform that sustains glycolytic energy metabolism in most tumor cells[34]. PKM2 can be regulated at multiple levels, including the transcriptional, posttranscriptional, and translational levels. For example, in prostate cancer, β-Arrestin2 induces PKM2 expression in a posttranscriptional manner through an hnRNP A1-dependent mechanism of alternative PKM splicing. This process significantly reduces the sensitivity of prostate cancer cells to docetaxel treatment[35]. Therefore, exploring the role of glycolysis in drug sensitivity and its regulatory mechanisms is crucial for understanding the development of drug resistance in CRC cells.

In this study, we found that SIRT1 expression is downregulated in oxaliplatin-resistant CRC cells and is correlated with the OS rates of CRC patients. Oxaliplatin-induced DNA damage activates PARP, leading to NAD⁺ depletion, which in turn inhibits SIRT1 expression. Alterations in the NAD⁺/SIRT1 pathway suggest a resistance mechanism. Inhibiting SIRT1 expression in CRC cells enhances oxaliplatin resistance, whereas enhancing SIRT1 activity increases the sensitivity of resistant CRC cells to oxaliplatin. Additionally, the expression of the glycolysis-related protein PKM2 is upregulated in resistant cells. The inhibition of SIRT1 promotes glycolysis in CRC cells, while the inhibition of glycolysis can reverse the enhanced oxaliplatin resistance caused by SIRT1 downregulation.

MATERIALS AND METHODS

Cell culture

The human CRC cell line HCT116-WT and the oxaliplatin-resistant HCT116 cell line HCT116 Oxa-R were obtained from Zhejiang Meisen Biotechnology (Zhejiang, China). These cells were cultured in DMEM (Gibco, Thermo Fisher Scientific, Waltham, MA, United States) supplemented with 10% fetal bovine serum (HyClone, Cytiva, Marlborough, MA, United States) and 1% penicillin/streptomycin (HyClone, Cytiva, Marlborough, MA, United States) at 37 °C in a humidified incubator containing 5% CO₂. Both cell lines were subjected to short tandem repeat profiling for authentication. To maintain the drug-resistant phenotype, the HCT116 Oxa-R cells were preserved in medium containing 20 μM oxaliplatin (Selleck, Houston, TX, United States).

Western blot

Total protein was isolated using RIPA lysis buffer (Thermo Fisher Scientific, Waltham, MA, United States) supplemented with PMSF (Sigma-Aldrich, St Louis, MO, United States). The protein concentration was determined *via* a bicinchoninic acid assay. Following 10% SDS-PAGE, the proteins were transferred to PVDF membranes (MilliporeSigma, Burlington, MA, United States), which were blocked with 5% (w/v) skim milk at room temperature for 1 hour. The membranes were probed with anti-SIRT1 (1:1000, #ab18494, Abcam, Cambridge, United Kingdom), anti-β-actin (1:1000, A5316, Sigma, St Louis, MO, United States), anti-GAPDH (1:1000, #5174S, CST, Danvers, MA, United States), anti-PKM2 (1:1000, #3198, CST, Danvers, MA, United States), anti-phospho-histone H2A. X (Ser139) (1:1500, #29380-1-AP, Proteintech, Rosemont,

IL, United States), and anti-PARP1 (1:1000, #13371-1-AP, Proteintech, Rosemont, IL, United States), followed by incubation with the appropriate HRP-conjugated secondary antibody (anti-mouse IgG/anti-rabbit IgG, 1:5000, CST, Danvers, MA, United States). The intensity of the blots was quantified with software ImageJ and normalized to that of β -actin or GAPDH. Experiments were performed in triplicate and the results are presented as the mean \pm SD.

Cell viability assay

To detect the sensitivity of CRC cells to oxaliplatin, as regulated by multiple small molecule inhibitors and agonists *in vitro*, HCT116-WT and HCT116 Oxa-R cells were seeded into 96-well plates (Corning) at a density of 5000 cells/well; the medium was removed 24 hours after the cells had time to equilibrate. The cells were then further cultured for 48 hours with medium containing various concentrations of oxaliplatin alone or in combination with various pathway regulators at appropriate concentrations. Cell viability was determined *via* a CellTiter96 Aqueous Non-Radioactive Cell Proliferation Assay Kit (Promega, Madison, WI, United States). The 3-(4,5-Dimethylthiazol2-yl)-5-(3-carboxymethoxyphenyl)-2-(4-sulfophenyl)-2H-tetrazolium, inner salt (MTS) solution was added to each well, after which the cells were incubated for 1 hour at 37 °C and 5% CO₂. The optical density (OD) was then measured at 490 nm with a microplate reader (Biotek Instruments, VT, United States). Cell viability was calculated using the following formula: (OD of treatment - OD of blank control)/(OD of control - OD of blank control) \times 100%.

Drug combination effect analysis

To investigate the synergistic effect between salermide and oxaliplatin, a drug combination assay was performed on HCT116 Oxa-R cells. Cells were exposed to drugs in non-constant ratio combinations for 24 hours. The combination index (CI) was calculated *via* Compusyn software (Biosoft, Ferguson, MO, United States), selecting the non-constant ratio option to evaluate the interaction between the two drugs. A CI value of less than 1 suggests a synergistic effect, a CI value equal to 1 indicates an additive effect, and a CI value greater than 1 indicating antagonism. The synergy scores and drug combination effects were visualized using SynergyFinder software, based on the (zero interaction potency) ZIP model. The dose-response matrix data were analyzed, and the ZIP synergy scores were calculated with SynergyFinder. A ZIP synergy score less than -10 is considered indicative of a synergistic interaction between the two drugs.

Transcriptome sequencing

HCT116-WT and HCT116 Oxa-R cells were cultured in 60 mm culture dishes until they reached 80%-90% confluence. Target cells in the logarithmic growth phase were collected, and total RNA was extracted for transcriptome sequencing and analysis, which were performed by Wuhan MetWare Biotechnology Co., Ltd.

NAD+ assay

The cells were cultured in six-well plates and divided into control, oxaliplatin-treated, rucaparib phosphate, and oxaliplatin + rucaparib phosphate groups, which were subjected to drug treatments for 24 hours. After reaching the appropriate state, the cells were washed three times with phosphate-buffered saline (PBS), digested with serum-free medium, and incubated with a fluorescent probe from the Cell Meter™ Intracellular NADH/NADPH Fluorescence Imaging Kit for 60 minutes. After staining, the cells were washed again three times with PBS. The fluorescence intensity was then measured by flow cytometry *via* the PE channel, and the fluorescence signals were recorded for each group.

Colony formation

To determine the colony formation ability of the cells, HCT116-WT and HCT116 Oxa-R cells and their derivative cells were seeded in 12-well plates (3 wells/treatment condition) at predetermined densities for each cell line and treated as indicated in the figure legends. The cells were cultured for 14 days and photographed after they were stained with crystal violet (0.5% w/v) in PBS supplemented with 25% methanol.

Measurement of extracellular acidification rates

In all, 2×10^5 cells were seeded into XF96 cell culture plates in complete Seahorse XF DMEM and incubated at 37 °C overnight in a humidified incubator with 5% CO₂. To equilibrate the temperature and pH of the detection system, the cells were washed with Seahorse XF DMEM and incubated at 37 °C for 1 hour in a CO₂-free incubator. An Agilent Seahorse XFe96 extracellular flux analyzer (Agilent Technologies, United States) was used to measure the extracellular acidification rate (ECAR). To assess glycolytic activity, the cells were treated with the Seahorse XF Glycolytic Rate Assay Kit, while glucose (100 mmol/L), oligomycin (10 μ M), and 2-deoxy-D-glucose (2-DG, 500 mmol/L) were added sequentially.

In vivo xenograft studies

All animal experiments were approved by the Animal Control Committee of the National Cancer Center/National Clinical Research Center for Cancer/Cancer Hospital of the Chinese Academy of Medical Sciences and Peking Union Medical College (NCC2024A242). The minimum sample size per group was calculated using the formula based on published literature: Minimum n = degrees of freedom (DF)/ k + 1 (For one-way ANOVA, the DF were set between 10 and 20). With DF = 10 and k = 4 groups, the minimum sample size per group was 4[36]. Twenty 5-6-week-old female BALB/c nude mice were used for the *in vivo* experiment. Resistant colon cancer cells (1×10^6 /mouse) were injected subcutaneously into the mice to establish a nude mouse tumor model. When the tumors reached approximately 300 mm³ in size, the nude mice were randomly divided into four groups (n = 5/group): The control group, oxaliplatin group, CAY10602 group, and oxaliplatin combined with CAY10602 group for drug treatment. Tumor length and width were

measured every three days for the continuous monitoring of tumor growth. The tumor volume was calculated according to the formula (length × width²) / 2. The experiment was terminated when the tumor volume reached 1500 mm³. Tumors were dissected, weighed, and fixed in formalin for subsequent analysis.

Analysis of SIRT1 expression and survival analysis in CRC using the Cancer Genome Atlas data

RNA-seq-based database containing gene expression matrix of 513 CRC cases and relevant clinical data, including treatment type, tumor stage, and OS, were downloaded from the Cancer Genome Atlas (TCGA) database. The differences in SIRT1 expression levels across different tumor stages (stage 1-stage 4) were examined using ANOVA. Kaplan-Meier survival analysis was used to compare OS between high ($n = 32$) and low expression ($n = 32$) groups in patients undergoing adjuvant chemotherapy.

Identification of differentially expressed genes

Patients datasets from TCGA database were classified into high ($n = 257$) and low ($n = 256$) SIRT1 expression groups based on SIRT1 mRNA levels. Gene expression was normalized using FPKM and subsequently transformed with a log₂-based approach transformation. Differential gene expression analysis between the high and low SIRT1 expression groups was conducted using the limma package in R program, with a significance threshold of $P < 0.05$ and a log₂ fold change (LogFC) greater than 0.5 or less than -0.5 as the criteria for selection.

Gene Ontology analysis and Gene Set Enrichment analysis

The ClusterProfiler package in R program was employed to analyze the Gene Ontology (GO) functions of differentially expressed genes (DEGs), aiming to identify potential SIRT1-related signaling pathways. Expression profiles of high and low SIRT1 expression groups were analyzed using Gene Set Enrichment analysis (GSEA) software. The analysis used the c2.cp.kegg_medicus.v2024.2.Hs.symbols.gmt gene set database with 1000 permutations, a permutation type of phenotype, and selection criteria of $P < 0.05$ and $| \text{normalized enrichment scores} | > 1$.

Statistical analysis

Statistical analysis was performed via GraphPad Prism 7 software, and images were generated via Adobe Photoshop CC 2020. Group comparisons were analyzed using the unpaired Student's *t* test and one-way ANOVA, with differences considered statistically significant when $P < 0.05$.

RESULTS

Identification of SIRT1 as a key regulator of oxaliplatin resistance in CRC

To explore the mechanism of oxaliplatin resistance in CRC, we utilized transcriptome sequencing technology to examine the transcriptome data of the parental human CRC cell line HCT116-WT and the oxaliplatin-resistant CRC cell line HCT116 Oxa-R. In all, 1928 DEGs were identified ($P < 0.05$, $| \log_{2}\text{FC} | > 1$; **Figure 1A**). To further investigate the resistance mechanism and to identify potential drug targets, we used the DEGs as query objects and entered them into the LINCS database for further analysis. By evaluating the similarity between the expression profiles of resistance-related DEGs and known small-molecule drugs in the database, we obtained a series of small-molecule drugs that are positively correlated with gene expression changes associated with oxaliplatin resistance in CRC. These molecules include: CHR2979, which inhibits nucleotide biosynthesis; perhexiline maleate, which inhibits fatty acid oxidation; Ro 28-1675, a protein tyrosine kinase inhibitor; and Amsacrine, a DNA topoisomerase II inhibitor. The screening results revealed the potential mechanism of oxaliplatin resistance in CRC. Among the small molecules, salermide, which is a known small-molecule inhibitor of SIRT1 (**Figure 1B**), was the tenth most common. Survival analysis of SIRT1 was conducted in the TCGA CRC cohort, and the results revealed a significant correlation between low SIRT1 expression and poor prognosis in *p53*-mutant CRC patients (**Figure 1C**). Further experimental results from Western blot experiments indicated that the expression level of SIRT1 was significantly downregulated in oxaliplatin-resistant CRC cells (**Figure 1D**). These results suggest that SIRT1 may play an important regulatory role in the development and treatment of CRC and that its low expression may be associated with resistance-related tumor progression.

PARP inhibition reverses oxaliplatin-induced downregulation of SIRT1 expression and decreases NAD⁺ levels

When cells experience DNA damage, the DNA damage repair enzyme PARP is activated to repair the DNA, a process which requires significant amounts of NAD⁺. Western blot analysis was performed to explore the state of DNA damage and repair pathways in HCT116-WT cells and HCT116 Oxa-R cells. The results revealed that the expression of the DNA damage marker γH2AX and the DNA damage repair enzyme PARP was significantly greater in HCT116 Oxa-R cells than in HCT116 Oxa-R cells (**Figure 2A**). The Western blot results also revealed that treatment with oxaliplatin (40 or 80 μM) for 12 or 24 hours led to a decrease in SIRT1 expression in HCT116 Oxa-R CRC cells (**Figure 2B**). Flow cytometry analysis revealed that the NAD⁺ levels in HCT116-WT cells were lower than those in HCT116 Oxa-R cells. Treatment of HCT116 Oxa-R cells with oxaliplatin (80 μM) caused a decrease in intracellular NAD⁺ levels, whereas treatment with rucaparib (5 μM) resulted in PARP inactivation in HCT116 Oxa-R cells, which reversed the intracellular NAD⁺ depletion induced by oxaliplatin (**Figure 2C**) and restored the low expression state of SIRT1 (**Figure 2D**). These results suggest that oxaliplatin treatment reduces intracellular NAD⁺ levels and suppresses SIRT1 expression by activating PARP.

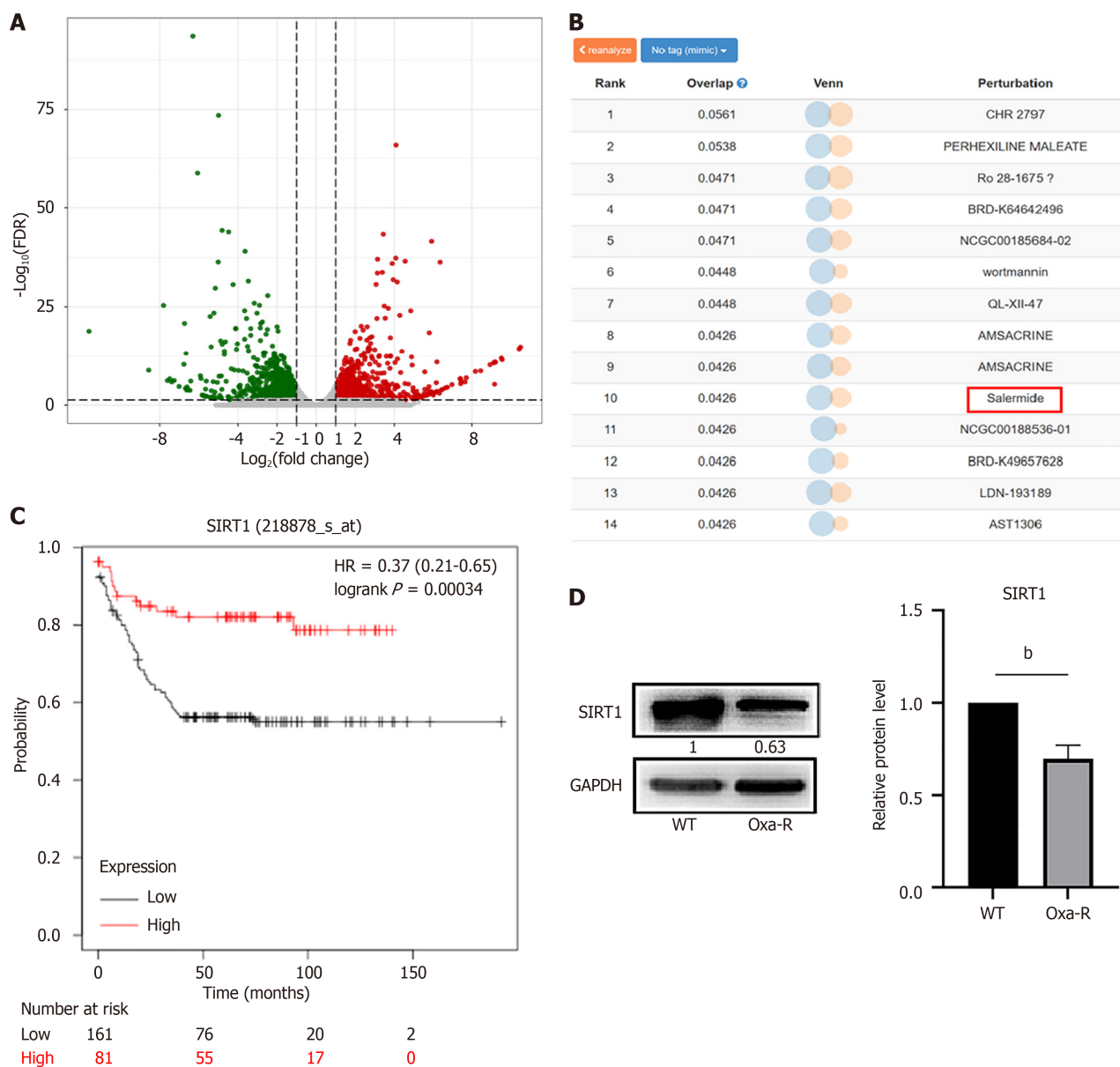


Figure 1 Screening of key molecules that regulate oxaliplatin resistance in colorectal cancer. A: Differentially expressed genes between HCT116 WT and HCT116 Oxa-R cells are shown in a volcano plot. In this plot, red dots represent upregulated differentially expressed genes, whereas green dots represent downregulated differentially expressed genes; B: Based on the expression profile of resistance-related differentially expressed genes, the Library of Integrated Network-based Cellular Signatures database was queried to identify small molecules with connectivity scores that are positively correlated with the resistance profile. These candidate drugs likely target mechanisms or pathways involved in regulating oxaliplatin resistance; C: The expression of *SIRT1* mRNA were associated with overall survival in colorectal cancer patients with *p53* mutations; D: Western blotting was performed to detect the expression levels of *SIRT1* in both HCT116-WT cells and HCT116 Oxa-R cells. Each bar represents means \pm SD of three separate experiments. ^b $P < 0.01$.

Inhibition of SIRT1 enhances oxaliplatin resistance in CRC cells

To assess the drug sensitivity of HCT116-WT and HCT116 Oxa-R cells to oxaliplatin, we measured the IC₅₀ values of oxaliplatin in these cells. The results of the MTS assay revealed that the IC₅₀ value of oxaliplatin in HCT116 Oxa-R cells (187.6 μ M) was significantly greater than that in HCT116-WT cells (8.248 μ M) (Figure 3A). Inhibition of SIRT1 expression increased the IC₅₀ value of oxaliplatin in HCT116 Oxa-R cells. The MTS results indicated that SIRT1 knockdown in HCT116 Oxa-R cells (IC₅₀ = 271.4 μ M) led to a significant increase in the IC₅₀ value of oxaliplatin, whereas overexpression of SIRT1 in HCT116 Oxa-R cells (IC₅₀ = 100.5 μ M) resulted in a significant decrease in the IC₅₀ value of oxaliplatin (Figure 3B). We treated HCT116 Oxa-R cells with different concentrations of the SIRT1 inhibitor salermide (0, 10, 20, or 40 μ M) and oxaliplatin (0, 10, 20, 40, 80, 160, or 320 μ M) and measured the absorbance in each well within 24 hours posttreatment according to the MTS assay to calculate the inhibition rate. The synergy score for the combined use of oxaliplatin and salermide was calculated via SynergyFinder software, with scores less than -10 indicating antagonism (Figure 3C). The inhibition rates of HCT116 Oxa-R cells treated with various combinations of oxaliplatin and salermide were analyzed via Cpmplusyn software to calculate the CI values. Analyses of the CI suggested that most of the data points were positioned below the line of additive effects (CI = 1) (Figure 3D). These findings indicate an antagonistic effect between salermide and oxaliplatin, which suggests that inhibition of SIRT1 expression may reduce the therapeutic

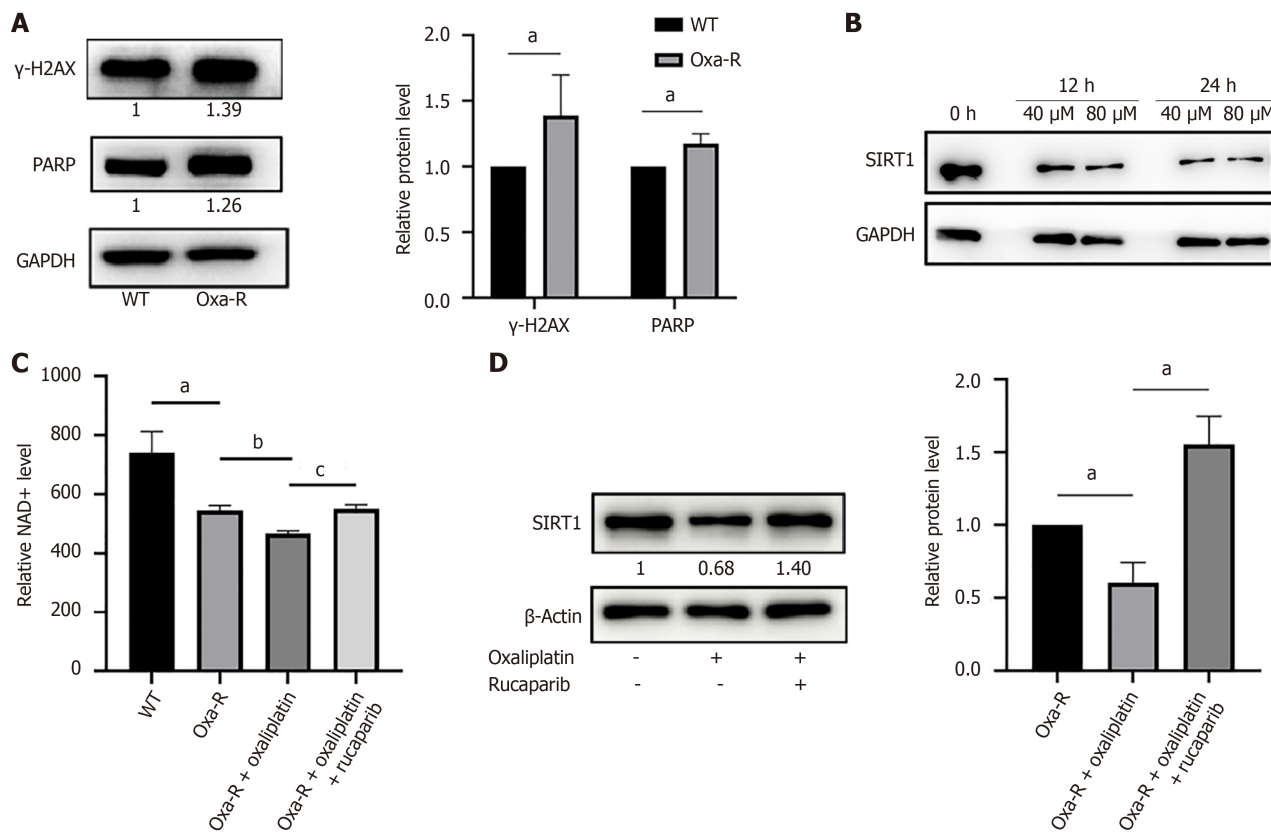


Figure 2 DNA damage induces NAD⁺ depletion and inhibits SIRT1 expression. **A:** Western blot analysis of γ-H2AX and PARP expression in HCT116 WT and HCT116 Oxa-R cells. Each bar represents means ± SD of three separate experiments. ^aP < 0.05. β-Actin was used as the internal reference; **B:** Western blot analysis shows SIRT1 expression in HCT116 Oxa-R cells treated with different concentrations of oxaliplatin (40, 80 μM) for 12 or 24 hours. GAPDH was used as the internal reference; **C:** Flow cytometry results indicate that NAD⁺ levels are lower in HCT116 Oxa-R cells than in HCT116-WT cells. Treatment with oxaliplatin (40 μM) for 12 hours induced NAD⁺ depletion in HCT116 Oxa-R cells, whereas treatment with rucaparib (5 μM) for 12 hours inactivated PARP and reversed oxaliplatin-induced NAD⁺ depletion. The data are presented as the means ± SD. ^aP < 0.05; ^bP < 0.01; ^cP < 0.001; **D:** Treatment with rucaparib (5 μM) for 12 hours reversed the oxaliplatin-induced reduction in SIRT1 expression. Each bar represents means ± SD of three separate experiments. ^aP < 0.05.

efficacy of oxaliplatin.

CAY10602 enhances oxaliplatin efficacy in HCT116 Oxa-R cells

To further explore strategies to overcome oxaliplatin resistance in CRC, we conducted colony formation assays, cell viability assays, and subcutaneous xenograft experiments in nude mice. MTS assay results revealed that inhibiting SIRT1 expression increased oxaliplatin resistance in HCT116 Oxa-R cells, whereas enhancing SIRT1 expression reduced oxaliplatin resistance in these cells (Figure 4A and B). The colony formation assay results indicated that CAY10602 (20 μM) enhanced the growth inhibitory effect of oxaliplatin (40 μM) on HCT116 Oxa-R cells (Figure 4C). Subcutaneous xenograft experiments in nude mice confirmed that the SIRT1 activator CAY10602 enhanced the growth-inhibitory effect of oxaliplatin on HCT116 Oxa-R cells (Figure 4D-F).

Increased glycolysis in HCT116 Oxa-R cells

To further explore the mechanism of resistance, we performed an enrichment analysis on the DEGs associated with resistance. The findings revealed that these genes are predominantly enriched in pathways such as the p53 signaling pathway, the PI3K-Akt signaling pathway, the MAPK signaling pathway, and cytokine-cytokine receptor interaction pathways. Particularly noteworthy is the glycolytic process, which ranks first among the metabolism-related enriched KEGG pathways (Figure 5A). Western blot analysis revealed notable upregulation of the expression of the key glycolytic enzymes PKM2 and LDHA in HCT116 Oxa-R cells relative to that in HCT116-WT cells (Figure 5B). The Seahorse glycolytic rate assay revealed a significantly greater ECAR in Oxa-R HCT116 cells than in WT HCT116 cells (Figure 5C). Collectively, these results indicate that an increase in the glycolytic metabolic pathway in resistant cells potentially confers a survival advantage.

SIRT1 affects drug resistance by regulating glycolysis

A correlation analysis was performed on the expression of SIRT1 and PKM2 based on the CRC gene expression data in the TCGA database. The results revealed that the levels of PKM2 and SIRT1 mRNA was significantly negatively correlated ($P < 0.05$, $R = -0.21$; Figure 6A). Western blot analysis revealed that the inhibition of SIRT1 expression can increase the expression levels of the key glycolytic enzymes PKM2 and LDHA in HCT116 Oxa-R cells, whereas an

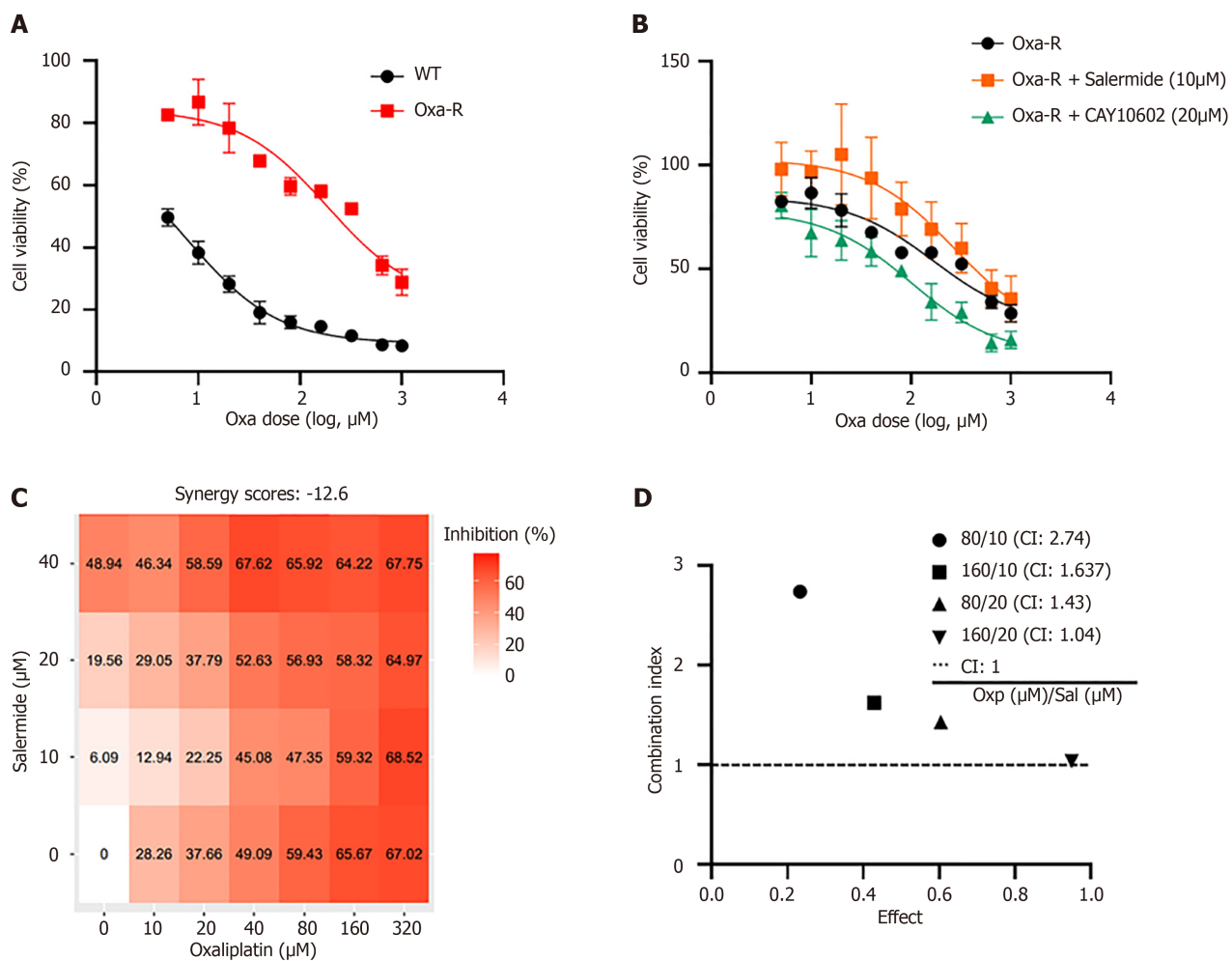


Figure 3 SIRT1 expression regulates the sensitivity of HCT116 Oxa-R cells to oxaliplatin. A: MTS assay was performed to determine the IC_{50} of oxaliplatin in HCT116-WT and HCT116 Oxa-R cells; B: HCT116 Oxa-R cells were treated with salermide (10 μM) to inhibit SIRT1 expression or CAY10602 (20 μM) to increase SIRT1 expression. Cell survival curves revealed that inhibition of SIRT1 increased the IC_{50} of oxaliplatin in HCT116 Oxa-R cells, whereas an increase in SIRT1 expression decreased the IC_{50} ; C: SynergyFinder software was used to calculate the synergy score for the combination of oxaliplatin and salermide in HCT116 Oxa-R cells (a score > 10 indicates synergy, -10 to 10 indicates additive effects, and < -10 indicates antagonism); D: Compusyn software was used to evaluate the combination index (CI) for oxaliplatin and salermide in HCT116 Oxa-R cells (CI < 1 indicates synergy, CI > 1 indicates antagonism, and CI = 1 indicates additive effects). CI: Combination index.

increase in SIRT1 expression can reduce the expression levels of these enzymes (Figure 6B). A Seahorse glycolytic rate assay revealed that inhibition of SIRT1 expression can increase the ECAR of HCT116 Oxa-R cells, which indicates that the glycolytic activity of these cells is increased. In contrast, enhancing SIRT1 expression reduced the ECAR in HCT116 Oxa-R cells, which indicates attenuated glycolytic activity (Figure 6C). These results demonstrate that SIRT1 can regulate the function of glycolysis, which may be one of the mechanisms by which this protein regulates drug resistance. To further elucidate the role of glycolysis in oxaliplatin resistance in CRC, we used shikonin (1 μM) to inhibit glycolysis in drug-resistant cells. MTS assay results revealed that inhibition of glycolysis in drug-resistant cells could reduce the oxaliplatin resistance of HCT116-WT cells and HCT116 Oxa-R cells (Figure 6D). In addition, the use of shikonin to inhibit glycolysis in drug-resistant cells reversed the increase in drug resistance caused by SIRT1 inhibition (Figure 6E and F). In summary, glycolysis is involved in the regulation of SIRT1-mediated oxaliplatin resistance in HCT116 Oxa-R cells.

Prognostic value of SIRT1 in CRC patients undergoing adjuvant chemotherapy and its potential molecular mechanisms

In the TCGA database, CRC patients were classified into four stages based on disease progression. To analyze the impact of SIRT1 on CRC progression, the levels of *SIRT1* mRNA were measured according to these tumor stages. The results showed that levels of *SIRT1* mRNA were significantly decreased in stage 4 compared to stages 1-3 (Figure 7A). Kaplan-Meier analysis revealed that CRC patients receiving adjuvant chemotherapy with lower *SIRT1* mRNA levels had significantly poorer OS compared to those with higher *SIRT1* mRNA levels ($P = 0.028$; Figure 7B). Differential expression analysis identified 553 DEGs (294 upregulated and 259 downregulated) between the high and low *SIRT1* mRNA expression groups (Figure 7C). To investigate the molecular pathways affected by SIRT1, GO analysis of the identified DEGs indicated involvement in ribosomal subunit, mitochondrial protein-containing complex, respiratory chain complex (Figure 7D). Furthermore, GSEA showed that the electron transfer in complex IV pathway was significantly enriched in

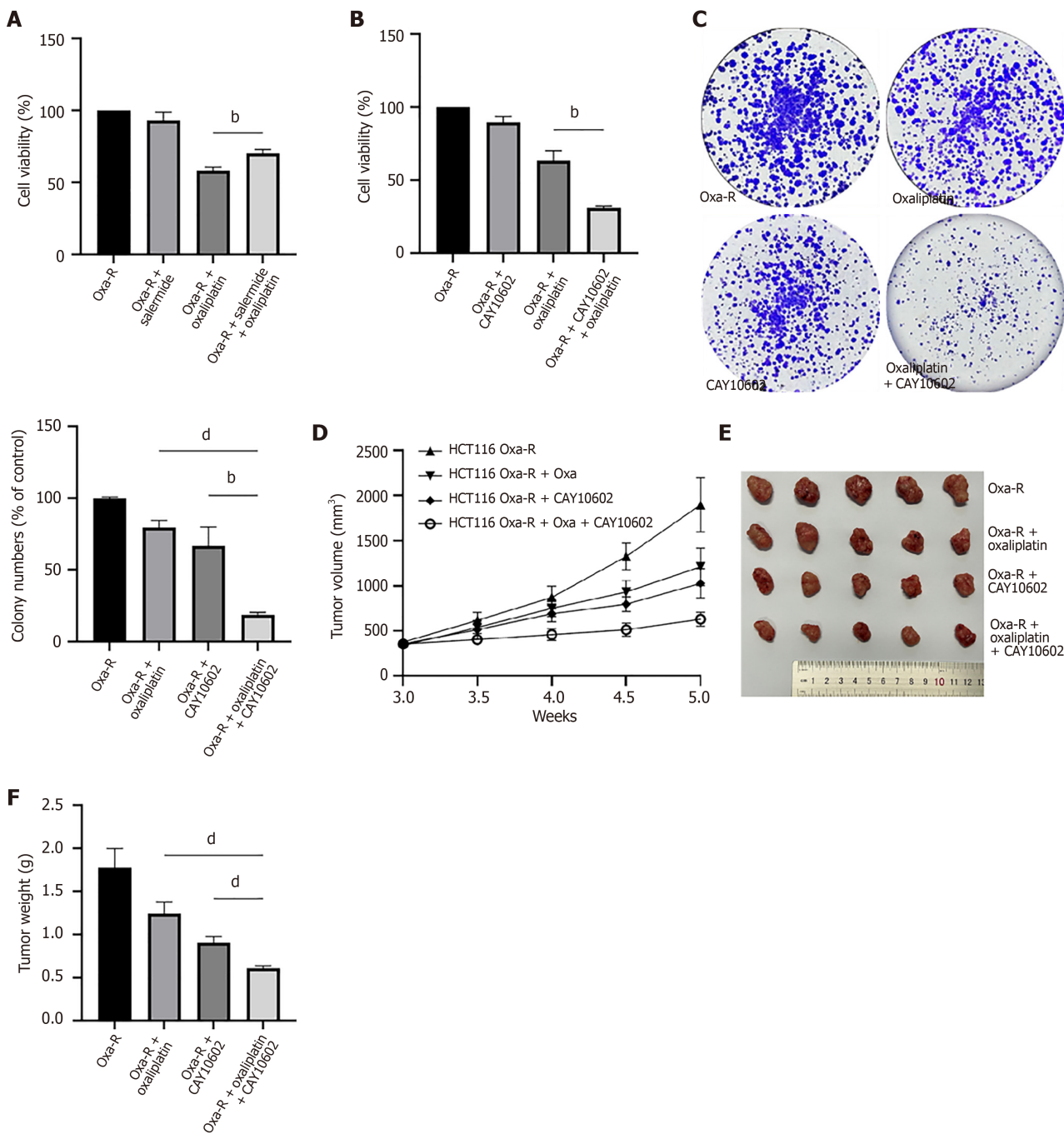


Figure 4 CAY10602 enhances the sensitivity of resistant cells to oxaliplatin. A: MTS results after 24 hours of treatment of HCT116 Oxa-R cells with oxaliplatin (40 μ M) alone, salermide (10 μ M) alone, or oxaliplatin combined with salermide. $^bP < 0.01$; B: MTS results after 24 hours of treatment of HCT116 Oxa-R cells with oxaliplatin (40 μ M) alone, CAY10602 (20 μ M) alone, or oxaliplatin combined with salermide. $^bP < 0.01$; C: Colony formation assay confirmed the inhibitory effect of 14 days of treatment with oxaliplatin (40 μ M) alone, CAY10602 (20 μ M) alone, or oxaliplatin combined with salermide in HCT116 Oxa-R cells. $^bP < 0.01$; $^dP < 0.0001$; D-F: Effect of CAY10602 on oxaliplatin resistance in subcutaneously implanted HCT116 Oxa-R cells in a nude mouse model (1×10^6 /mouse; $n = 5$ /group). Tumors harvested from these nude mice were treated with saline (control), oxaliplatin alone (10 mg/kg, three times a week), CAY10602 alone (10 mg/kg, three times a week) or oxaliplatin together with CAY10602. The tumor volumes were quantified as $V = L \times W^2/2$ (where L is the length and W is the width). Tumors were harvested when the diameter was > 1.5 cm. $^dP < 0.0001$.

the low SIRT1 mRNA expression group (Figure 7E). These findings suggested that reduced SIRT1 expression may influence chemoresistance by impacting the respiratory chain complex.

DISCUSSION

Significant progress has been made in the treatment of CRC over the past several decades, and this progress encompasses surgical interventions combined with local or systemic radiotherapy and chemotherapy supplemented with targeted

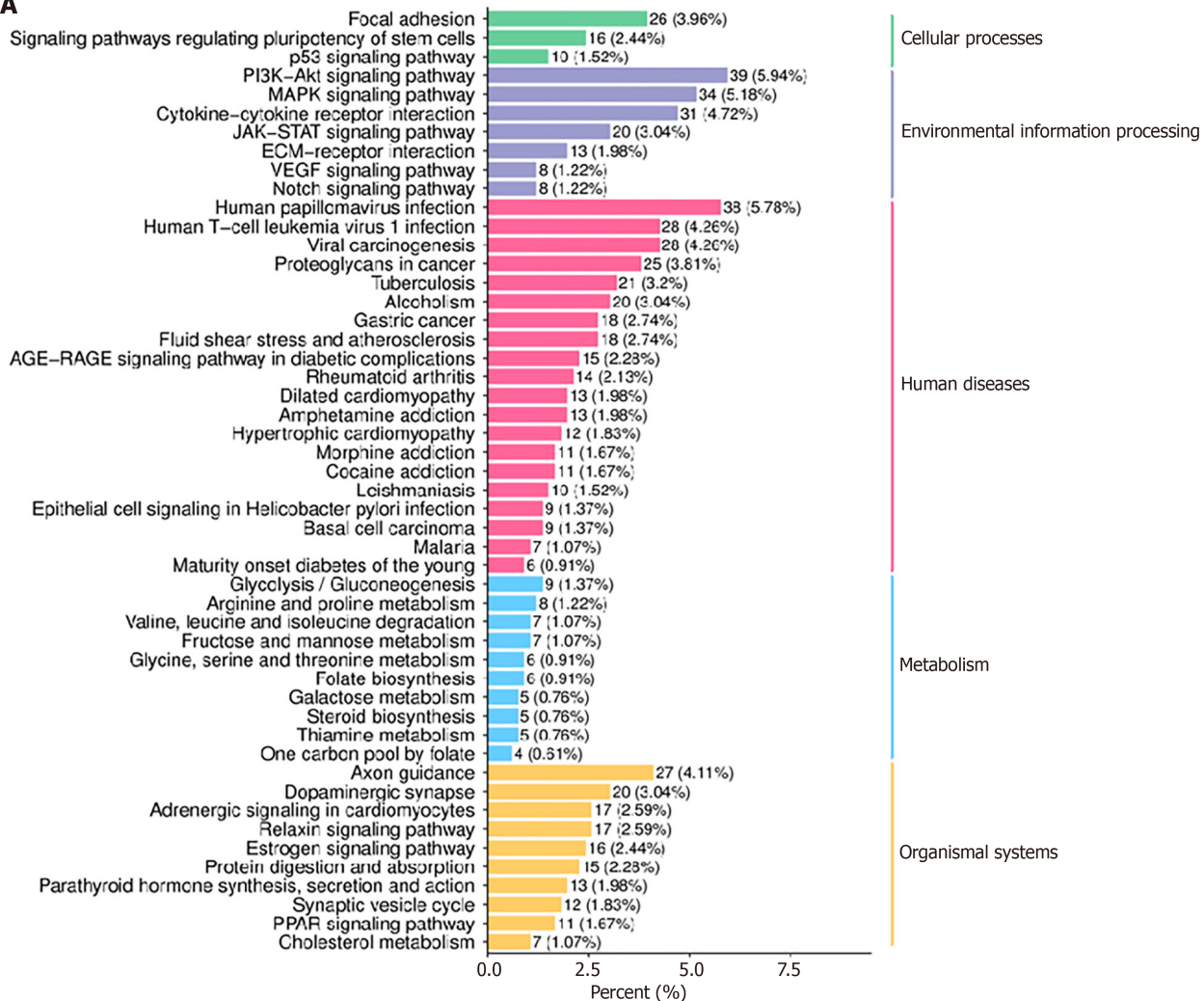
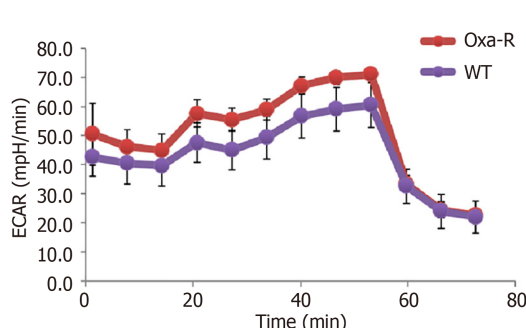
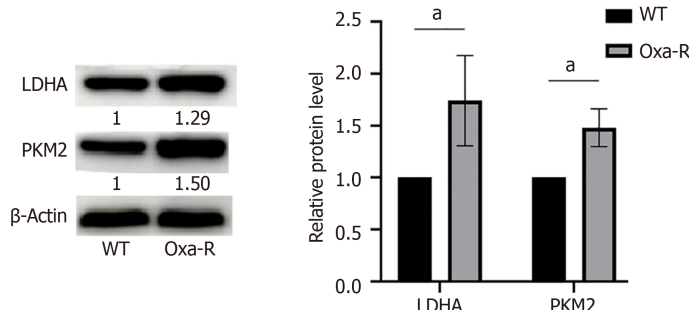
A**C****B**

Figure 5 Increased glycolysis in Oxa-R colorectal cancer cells. A: Enrichment analyses of the Kyoto Encyclopedia of Genes and Genomes pathways associated with resistance-related differentially expressed genes; B: Western blots to determine expression of the key glycolytic enzymes LDHA and PKM2 in HCT116-WT and HCT116 Oxa-R cells. Each bar represents means \pm SD of three separate experiments. $^aP < 0.05$. β -Actin was used as the internal reference; C: HCT116-WT and HCT116 Oxa-R cells were seeded in 96-well Seahorse assay plates, and glucose (100 mmol/L), oligomycin (10 μ M) and 2-DG (500 mmol/L) were successively added to measure the extracellular acidification rate.

therapies, radiotherapy, and immunotherapy. These treatments are usually determined according to the patient's physiological status and disease stage[37]. Chemotherapy is the primary treatment for patients with advanced and metastatic CRC, and the cytotoxic drug oxaliplatin is often a crucial component of both monotherapy and combination chemotherapy regimens[38]. Oxaliplatin-based chemotherapy is commonly used to treat patients at high risk of cancer recurrence or those with advanced or metastatic disease[39]. It is recommended that high-risk patients with stage II and III CRC undergo adjuvant chemotherapy with a combination of 5-FU and oxaliplatin after surgery to improve OS rates [40]. However, a significant portion of patients who receive oxaliplatin therapy develop chemoresistance during treatment, ultimately succumbing to tumor progression and recurrence[6,41]. The development of resistance is a multifactorial process that involves alterations in drug transport mechanisms[42], aggressive tumor growth, and the

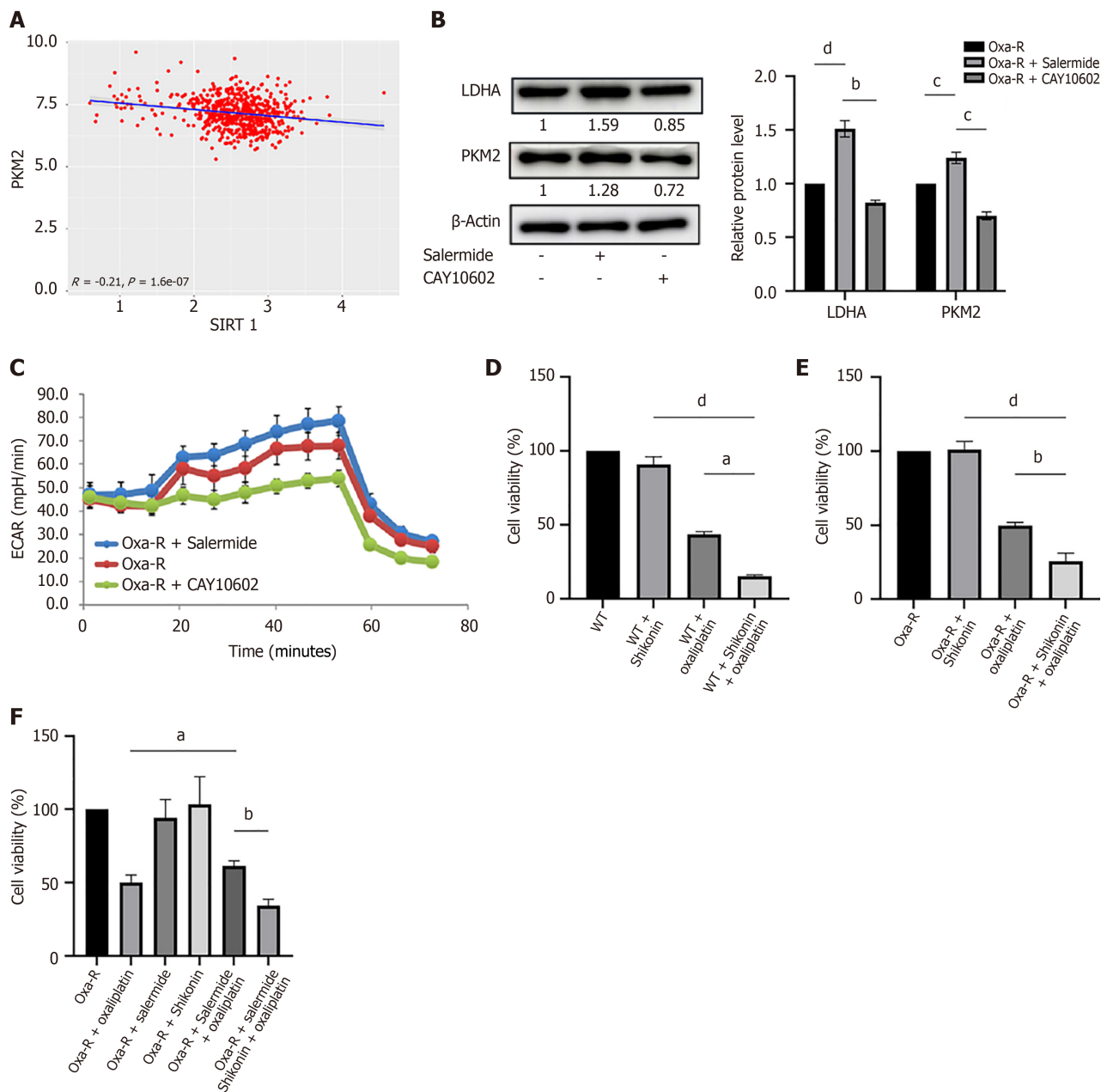


Figure 6 SIRT1 influences oxaliplatin resistance in colorectal cancer cells by regulating glycolysis. A: Analysis of the Cancer Genome Atlas data shows the correlation between SIRT1 and PKM2 expression in colorectal cancer; B: Western blot analysis revealed the expression of LDHA and PKM2 in HCT116 Oxa-R cells after treatment with salermide (10 μM) or CAY10602 (20 μM) for 12 hours. Each bar represents means ± SD of three separate experiments. ^aP < 0.01; ^bP < 0.001; ^cP < 0.0001. β-Actin served as the internal reference; C: Measurement of the extracellular acidification rate in HCT116 Oxa-R cells with increased or inhibited SIRT1 expression; D: MTS results after 24 hours of treatment of HCT116-WT cells with oxaliplatin (40 μM) alone, shikonin (1 μM) alone, or oxaliplatin combined with shikonin. ^aP < 0.05; ^dP < 0.0001; E: MTS results after 24 hours of treatment of HCT116 Oxa-R cells with oxaliplatin (40 μM) alone, shikonin (1 μM) alone, or oxaliplatin combined with shikonin. ^bP < 0.01; ^dP < 0.0001; F: A rescue experiment using the MTS assay was performed to evaluate the effect of glycolysis inhibition on the enhanced resistance to oxaliplatin caused by low SIRT1 expression. The Oxa-R cells were treated with oxaliplatin (40 μM) alone, shikonin (1 μM) alone, salermide (10 μM) alone, oxaliplatin (40 μM) combined with salermide (10 μM), or oxaliplatin (40 μM) combined with salermide (10 μM) and shikonin (1 μM) for 24 hours. ^aP < 0.05; ^bP < 0.01.

involvement of the tumor immune microenvironment[43]. This process is driven by a series of dysregulated genes, but the factors leading to platinum resistance and their application in clinical practice remain unclear[44]. To elucidate the relationships among gene expression, molecular mechanisms, and molecular phenotypes, many studies use the gene expression profiles of target diseases or resistance-related phenotypes as references. These profiles are compared with many drug-induced gene expression profiles (perturbation profiles) in the LINCS database, and similarity analysis of gene expression patterns are used to explore the correlations between drugs and phenotypes[45]. In our study, using a strategy that combines transcriptome sequencing data with LINCS data screening, we identified SIRT1 as a key regulatory molecule in oxaliplatin resistance in CRC.

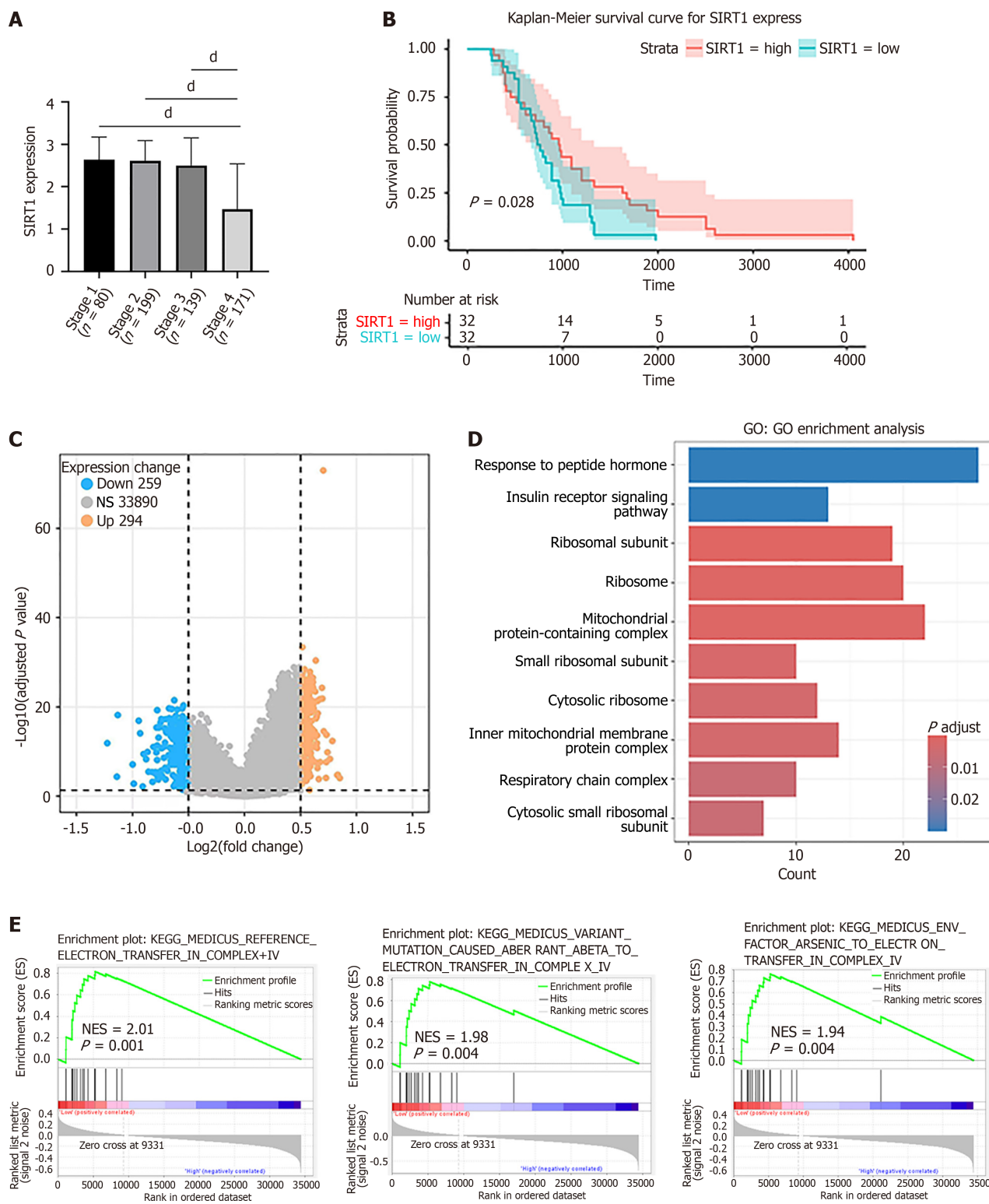


Figure 7 Integrated analysis expression, prognostic value and associated molecular pathways of SIRT1 in colorectal cancer. A: Relationships between SIRT1 mRNA levels and individual cancer stages of colorectal cancer (CRC). $\text{d}P < 0.0001$; B: Relationships between SIRT1 mRNA levels and overall survival of CRC patients undergoing adjuvant chemotherapy were conducted using Kaplan-Meier analysis; C: Volcano plot of differentially expressed genes in CRC patients with high and low SIRT1 mRNA expression. Yellow dots represent upregulated genes; blue dots represent downregulated genes; gray dots represent non-significant genes; D: Gene Ontology functional enrichment analysis of differentially expressed genes; E: Gene Set Enrichment analysis in the low SIRT1 mRNA expression group. NES: Normalized enrichment scores.

Abnormal cancer cell metabolism provides a favorable environment for tumorigenesis and the development of drug resistance[46,47]. Under aerobic conditions, normal cells generate energy mainly through oxidative phosphorylation *via* oxygen-dependent pathways and through glycolysis under anaerobic conditions[48]. Cancer cells tend to use glycolysis to produce energy and metabolites; that is, under aerobic conditions, glucose is preferentially converted into pyruvate in the cytoplasm and then further converted into lactic acid[49]. This phenomenon is called the Warburg effect. Glycolysis enhances the growth advantage of tumor cells through multiple pathways: (1) Many intermediates (including nucleic acids, lipids, and proteins) produced during the glycolysis metabolic pathway serve as raw materials required for cancer cell proliferation. For example, the pentose phosphate pathway is a bypass formed from the intermediate product of glycolysis, glucose-6-phosphate, which mainly produces pentose phosphate for nucleic acid synthesis and NAD⁺ phosphate for fatty acid synthesis, thereby supporting tumor cell growth[50]; (2) By increasing glucose intake, tumor cells increase the rate of ATP production *via* glycolysis[51]; and (3) Increased glucose uptake by tumor cells can lead to increased glycolysis and inhibition of the mitochondrial tricarboxylic acid cycle (OXPHOS). When mitochondrial activity is inhibited, the electron transport chain is limited to ROS production, thereby reducing cell apoptosis. One study showed that β-hydroxybutyrate can inhibit glycolysis and direct the energy pathway to the tricarboxylic acid cycle, thereby enhancing the sensitivity of tumor cells to oxaliplatin and the efficacy of chemotherapy drugs through the production of ROS[52].

After entering the cell, glucose is broken down into lactate through the process of glycolysis and thus glucose consumption and lactate production usually reflect glycolysis (Mou *et al*[53], 2018). This process involves a series of enzymes involved in catalytic reactions, and enzymes that directly promote glycolysis usually also promote drug resistance in tumor cells[54]. PKM2, a PK and the final rate-limiting enzyme of glycolysis, can transfer the phosphate group in phosphoenolpyruvate to ADP for internalization into pyruvate. Pyruvate is ultimately reduced to lactate by LDHA[55]. In recent years, strategies targeting glycolytic metabolism have provided new ideas for cancer treatment. For example, hexokinase 2 (HK2) catalyzes the first rate-limiting step in glucose metabolism, and the HK2 inhibitor 2-DG can reverse drug resistance in multiple *in vitro* models[56]. Monocarboxylate transporter 1 (MCT1) is responsible for the transport of lactate, the main product of aerobic glycolysis in cells, and targeting MCT1 greatly enhances the sensitivity of human osteosarcoma cells to chemotherapy[57]. Our study revealed that glycolytic metabolism is enhanced in drug-resistant cells compared with parental cells. The SIRT1 agonist CAY10602 can inhibit the expression of PKM2, a key enzyme of glycolysis. Inhibition of glycolysis in CRC cells can reverse the enhanced oxaliplatin resistance induced by the SIRT1 inhibitor salermide. SIRT1 is a deacetylase that removes acetyl groups from lysine residues in histones and nonhistone proteins by consuming NAD⁺, thereby participating in the regulation of various biological processes, including gene transcription, apoptosis, cell cycle regulation, DNA damage repair, and metabolism. SIRT1 has significant impacts on cell proliferation, aging, and the stress response[58,59]. Increasing evidence suggests that SIRT1, as a major regulator of metabolic reprogramming, is involved in tumorigenesis and can serve as a biomarker of drug resistance and as a prognostic indicator in cancer patients[27,60]. For example, corydalis inhibits glycolysis and delays the progression of hepatic steatosis to hepatocellular carcinoma by activating the AMPK-SREBP-1c-SIRT1 axis in nonalcoholic fatty liver disease[61]. This study aimed to investigate the role of the NAD⁺/SIRT1 pathway in oxaliplatin resistance in CRC cells. Our results revealed a decrease in NAD⁺ levels and low expression of SIRT1 in resistant cells. Specifically, we found that the DNA repair enzyme PARP is overactivated in resistant cells, which leads to a reduction in the intracellular NAD⁺ level, thereby inhibiting SIRT1 expression. PARP inhibitors can reverse DNA damage repair-induced NAD⁺ depletion and SIRT1 downregulation. Numerous reports have demonstrated that PARP inhibitors, either alone or in combination with cytotoxic drugs, can be used to treat BRCA1/2-mutant breast cancers[62]. Similarly, p53-deficient breast cancer cells treated with PARP inhibitors lose resistance to anthracycline drugs, which promote apoptosis and exert antitumor activity[63]. Therefore, future studies should continue to investigate the combined use of SIRT1 agonists and PARP inhibitors to kill tumor cells and reverse drug resistance.

However, the study still has certain limitations. Firstly, this study explored the molecular mechanisms of SIRT1 based primarily on bioinformatics analysis. It requires further verification through *in vivo* and *in vitro* studies, such as gene knockout or knockdown experiments combined with proteomics and metabolomics analysis. Secondly, this study was conducted by sourcing data from TCGA, a database providing important insights into the correlation of SIRT1 expression with CRC progression and survival. Further studies should incorporate clinical samples (such as immunohistochemistry) to further validate our findings and assess the clinical value of SIRT1.

CONCLUSION

In this study, we investigated the changes in the NAD⁺/SIRT1 pathway in oxaliplatin-resistant CRC cells. We observed that NAD⁺ levels were decreased and that SIRT1 expression was downregulated in oxaliplatin-resistant cells. DNA damage activates the DNA repair enzyme PARP, which leads to NAD⁺ depletion and the suppression of SIRT1 expression. Inhibition of PARP can reverse the alterations in the NAD⁺/SIRT1 pathway caused by DNA damage. Additionally, we observed enhanced glycolysis in resistant cells. An increase in SIRT1 expression overcame oxaliplatin resistance in CRC cells and reduced their glycolytic activity. Glycolysis is also involved in the increased resistance induced by SIRT1 inhibition (Figure 8). These results suggest that SIRT1 acts as a metabolic regulator in the resistance process and that enhancing SIRT1 expression could be an effective strategy to reverse oxaliplatin resistance in CRC.

NAD+/SIRT1 Pathway

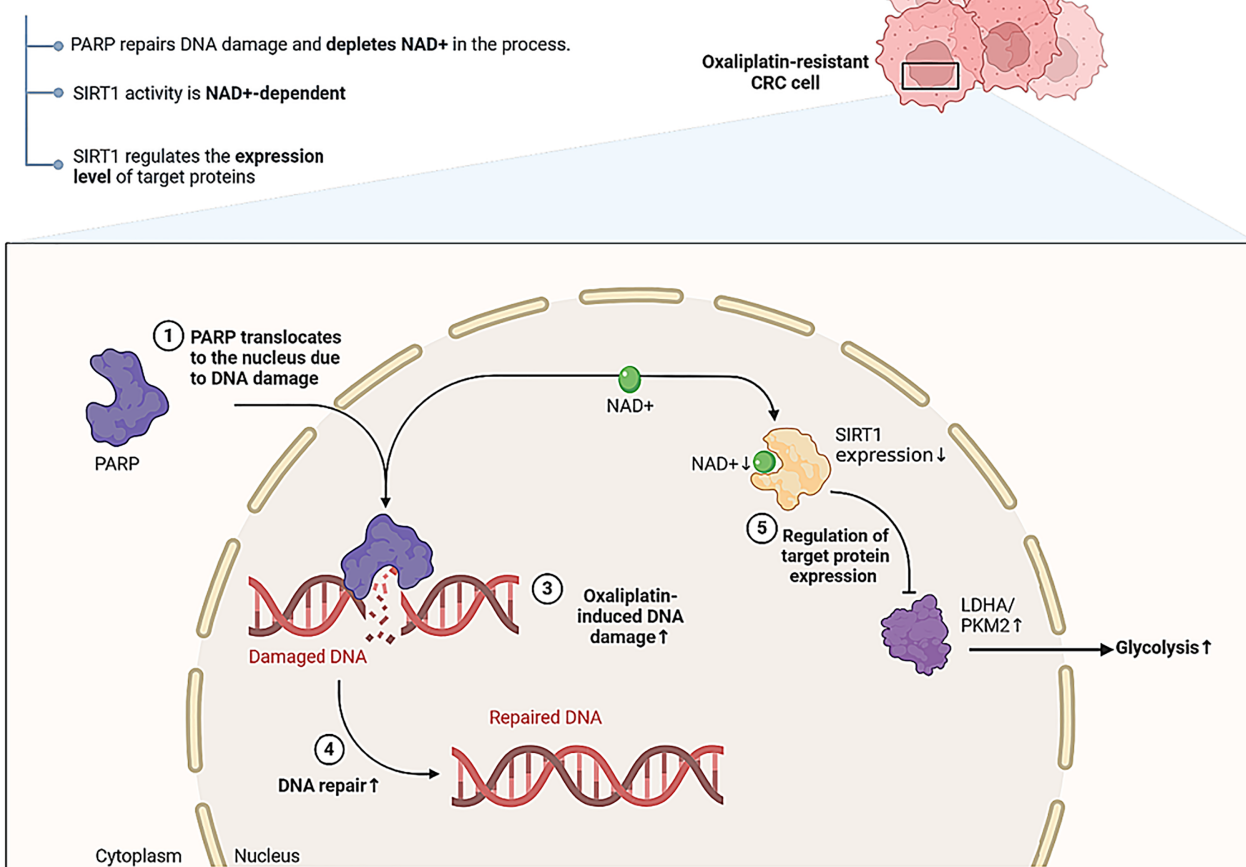


Figure 8 Schematic diagram of SIRT1 inhibition-driven glycolysis and oxaliplatin resistance in colorectal cancer cells. DNA damage, a crucial driver of increased glycolysis in colorectal cancer (CRC) cells, exerts its effect primarily through PARP activation, which depletes intracellular NAD+, thereby inhibiting SIRT1 expression. Enhanced glycolysis in CRC cells via SIRT1 inhibition, which contributes to oxaliplatin resistance. CRC: Colorectal cancer.

ACKNOWLEDGEMENTS

We appreciate the technical support provided by the Lab Platform of the National Cancer Center/National Clinical Research Center for Cancer/Cancer Hospital.

FOOTNOTES

Author contributions: Qian HL and Sun YK conceived the project and provided funding support for the experiments; Niu YR designed the study, performed the experiments and wrote the manuscript; Xiang MD collected the data and performed the data analysis; Yang WW and Fang YT assisted with data analysis and provided critical revisions; All the authors reviewed and approved the final manuscript.

Supported by the National Natural Science Foundation of China, No. 82072756; and Beijing Xisike Clinical Oncology Research Foundation, No. Y-HR2019-0285.

Institutional animal care and use committee statement: All animal experiments were approved by the Animal Control Committee of the National Cancer Center/National Clinical Research Center for Cancer/Cancer Hospital of the Chinese Academy of Medical Sciences and Peking Union Medical College (NCC2024A242).

Conflict-of-interest statement: All the authors report no relevant conflicts of interest for this article.

Data sharing statement: The relevant research data are included in the manuscript. Additional data will be made available upon request at hsunyk@cicams.ac.cn.

ARRIVE guidelines statement: The authors have read the ARRIVE guidelines, and the manuscript was prepared and revised according to the ARRIVE guidelines.

Open Access: This article is an open-access article that was selected by an in-house editor and fully peer-reviewed by external reviewers. It is distributed in accordance with the Creative Commons Attribution NonCommercial (CC BY-NC 4.0) license, which permits others to distribute, remix, adapt, build upon this work non-commercially, and license their derivative works on different terms, provided the original work is properly cited and the use is non-commercial. See: <https://creativecommons.org/Licenses/by-nc/4.0/>

Country of origin: China

ORCID number: Ya-Ru Niu 0000-0001-7880-4007; Wen-Wei Yang 0000-0002-7292-5980; Yong-Kun Sun 0000-0003-3302-6023.

S-Editor: Li L

L-Editor: A

P-Editor: Yu HG

REFERENCES

- 1 Sung H, Ferlay J, Siegel RL, Laversanne M, Soerjomataram I, Jemal A, Bray F. Global Cancer Statistics 2020: GLOBOCAN Estimates of Incidence and Mortality Worldwide for 36 Cancers in 185 Countries. *CA Cancer J Clin* 2021; **71**: 209-249 [PMID: 33538338 DOI: 10.3322/caac.21660]
- 2 Ciardiello F, Ciardiello D, Martini G, Napolitano S, Tabernero J, Cervantes A. Clinical management of metastatic colorectal cancer in the era of precision medicine. *CA Cancer J Clin* 2022; **72**: 372-401 [PMID: 35472088 DOI: 10.3322/caac.21728]
- 3 Ding K, Mou P, Wang Z, Liu S, Liu J, Lu H, Yu G. The next bastion to be conquered in immunotherapy: microsatellite stable colorectal cancer. *Front Immunol* 2023; **14**: 1298524 [PMID: 38187388 DOI: 10.3389/fimmu.2023.1298524]
- 4 Osterman E, Hammarström K, Imam I, Osterlund E, Sjöblom T, Glimelius B. Recurrence Risk after Radical Colorectal Cancer Surgery-Less Than before, But How High Is It? *Cancers (Basel)* 2020; **12**: 3308 [PMID: 33182510 DOI: 10.3390/cancers12113308]
- 5 Benson AB, Venook AP, Al-Hawary MM, Arain MA, Chen YJ, Ciombor KK, Cohen S, Cooper HS, Deming D, Farkas L, Garrido-Laguna I, Grem JL, Gunn A, Hecht JR, Hoffe S, Hubbard J, Hunt S, Johung KL, Kirilcuk N, Krishnamurthi S, Messersmith WA, Meyerhardt J, Miller ED, Mulcahy MF, Nurkin S, Overman MJ, Parikh A, Patel H, Pedersen K, Saltz L, Schneider C, Shibata D, Skibber JM, Sofocleous CT, Stoffel EM, Stotsky-Himelfarb E, Willett CG, Gregory KM, Gurski LA. Colon Cancer, Version 2.2021, NCCN Clinical Practice Guidelines in Oncology. *J Natl Compr Canc Netw* 2021; **19**: 329-359 [PMID: 33724754 DOI: 10.6004/jnccn.2021.0012]
- 6 Katona BW, Weiss JM. Chemoprevention of Colorectal Cancer. *Gastroenterology* 2020; **158**: 368-388 [PMID: 31563626 DOI: 10.1053/j.gastro.2019.06.047]
- 7 Underwood PW, Ruff SM, Pawlik TM. Update on Targeted Therapy and Immunotherapy for Metastatic Colorectal Cancer. *Cells* 2024; **13**: 245 [PMID: 38334637 DOI: 10.3390/cells13030245]
- 8 Guo Y, Wang M, Zou Y, Jin L, Zhao Z, Liu Q, Wang S, Li J. Mechanisms of chemotherapeutic resistance and the application of targeted nanoparticles for enhanced chemotherapy in colorectal cancer. *J Nanobiotechnology* 2022; **20**: 371 [PMID: 35953863 DOI: 10.1186/s12951-022-01586-4]
- 9 Luo S, Yue M, Wang D, Lu Y, Wu Q, Jiang J. Breaking the barrier: Epigenetic strategies to combat platinum resistance in colorectal cancer. *Drug Resist Updat* 2024; **77**: 101152 [PMID: 39369466 DOI: 10.1016/j.drup.2024.101152]
- 10 Luo ZD, Wang YF, Zhao YX, Yu LC, Li T, Fan YJ, Zeng SJ, Zhang YL, Zhang Y, Zhang X. Emerging roles of non-coding RNAs in colorectal cancer oxaliplatin resistance and liquid biopsy potential. *World J Gastroenterol* 2023; **29**: 1-18 [PMID: 36683709 DOI: 10.3748/wjg.v29.i1.1]
- 11 Song M, Huang S, Wu X, Zhao Z, Liu X, Wu C, Wang M, Gao J, Ke Z, Ma X, He W. UBR5 mediates colorectal cancer chemoresistance by attenuating ferroptosis via Lys 11 ubiquitin-dependent stabilization of Smad3-SLC7A11 signaling. *Redox Biol* 2024; **76**: 103349 [PMID: 39260061 DOI: 10.1016/j.redox.2024.103349]
- 12 Li Y, Gan Y, Liu J, Li J, Zhou Z, Tian R, Sun R, Liu J, Xiao Q, Li Y, Lu P, Peng Y, Peng Y, Shu G, Yin G. Downregulation of MEIS1 mediated by ELF1-AS1/EZH2/DNMT3a axis promotes tumorigenesis and oxaliplatin resistance in colorectal cancer. *Signal Transduct Target Ther* 2022; **7**: 87 [PMID: 35351858 DOI: 10.1038/s41392-022-00902-6]
- 13 Garcia-Mayea Y, Mir C, Masson F, Paciucci R, Lleonart ME. Insights into new mechanisms and models of cancer stem cell multidrug resistance. *Semin Cancer Biol* 2020; **60**: 166-180 [PMID: 31369817 DOI: 10.1016/j.semcancer.2019.07.022]
- 14 Li Q, Sun H, Luo D, Gan L, Mo S, Dai W, Liang L, Yang Y, Xu M, Li J, Zheng P, Li X, Li Y, Wang Z. Lnc-RP11-536 K7.3/SOX2/HIF-1α signaling axis regulates oxaliplatin resistance in patient-derived colorectal cancer organoids. *J Exp Clin Cancer Res* 2021; **40**: 348 [PMID: 34740372 DOI: 10.1186/s13046-021-02143-x]
- 15 Rottenberg S, Disler C, Perego P. The rediscovery of platinum-based cancer therapy. *Nat Rev Cancer* 2021; **21**: 37-50 [PMID: 33128031 DOI: 10.1038/s41568-020-00308-y]
- 16 Lord CJ, Ashworth A. The DNA damage response and cancer therapy. *Nature* 2012; **481**: 287-294 [PMID: 22258607 DOI: 10.1038/nature10760]
- 17 Cameron AM, Castoldi A, Sanin DE, Flachsmann LJ, Field CS, Puleston DJ, Kyle RL, Patterson AE, Hässler F, Buescher JM, Kelly B, Pearce EL, Pearce EJ. Inflammatory macrophage dependence on NAD(+) salvage is a consequence of reactive oxygen species-mediated DNA damage. *Nat Immunol* 2019; **20**: 420-432 [PMID: 30858618 DOI: 10.1038/s41590-019-0336-y]
- 18 Covarrubias AJ, Perrone R, Grozio A, Verdin E. NAD(+) metabolism and its roles in cellular processes during ageing. *Nat Rev Mol Cell Biol* 2021; **22**: 119-141 [PMID: 33535981 DOI: 10.1038/s41580-020-00313-x]
- 19 Xie N, Zhang L, Gao W, Huang C, Huber PE, Zhou X, Li C, Shen G, Zou B. NAD(+) metabolism: pathophysiologic mechanisms and therapeutic potential. *Signal Transduct Target Ther* 2020; **5**: 227 [PMID: 33028824 DOI: 10.1038/s41392-020-00311-7]
- 20 Anderson KA, Madsen AS, Olsen CA, Hirschev MD. Metabolic control by sirtuins and other enzymes that sense NAD(+), NADH, or their ratio. *Biochim Biophys Acta Bioenerg* 2017; **1858**: 991-998 [PMID: 28947253 DOI: 10.1016/j.bbabi.2017.09.005]
- 21 Vernousfaderani EK, Akhtari N, Rezaei S, Rezaee Y, Shiranirad S, Mashhadi M, Hashemi A, Khankandi HP, Behzad S. Resveratrol and

- Colorectal Cancer: A Molecular Approach to Clinical Researches. *Curr Top Med Chem* 2021; **21**: 2634-2646 [PMID: 34749615 DOI: 10.2174/156802662166211105093658]
- 22** **Bosch-Presegué L**, Vaquero A. The dual role of sirtuins in cancer. *Genes Cancer* 2011; **2**: 648-662 [PMID: 21941620 DOI: 10.1177/1947601911417862]
- 23** **Das N**, Mukherjee S, Das A, Gupta P, Bandyopadhyay A, Chattopadhyay S. Intra-tumor ROS amplification by melatonin interferes in the apoptosis-autophagy-inflammation-EMT collusion in the breast tumor microenvironment. *Heliyon* 2024; **10**: e23870 [PMID: 38226217 DOI: 10.1016/j.heliyon.2023.e23870]
- 24** **Ren NSX**, Ji M, Tokar EJ, Busch EL, Xu X, Lewis D, Li X, Jin A, Zhang Y, Wu WKK, Huang W, Li L, Fargo DC, Keku TO, Sandler RS, Li X. Haploinsufficiency of SIRT1 Enhances Glutamine Metabolism and Promotes Cancer Development. *Curr Biol* 2017; **27**: 483-494 [PMID: 28162896 DOI: 10.1016/j.cub.2016.12.047]
- 25** **Sun T**, Hu Y, He W, Shang Y, Yang X, Gong L, Zhang X, Gong P, Yang G. SRT2183 impairs ovarian cancer by facilitating autophagy. *Aging (Albany NY)* 2020; **12**: 24208-24218 [PMID: 33223507 DOI: 10.18632/aging.104126]
- 26** **Wang RH**, Sengupta K, Li C, Kim HS, Cao L, Xiao C, Kim S, Xu X, Zheng Y, Chilton B, Jia R, Zheng ZM, Appella E, Wang XW, Ried T, Deng CX. Impaired DNA damage response, genome instability, and tumorigenesis in SIRT1 mutant mice. *Cancer Cell* 2008; **14**: 312-323 [PMID: 18835033 DOI: 10.1016/j.ccr.2008.09.001]
- 27** **Wei Z**, Xia J, Li J, Cai J, Shan J, Zhang C, Zhang L, Wang T, Qian C, Liu L. SIRT1 promotes glucolipid metabolic conversion to facilitate tumor development in colorectal carcinoma. *Int J Biol Sci* 2023; **19**: 1925-1940 [PMID: 37063423 DOI: 10.7150/ijbs.76704]
- 28** **Guo F**, Xu F, Li S, Zhang Y, Lv D, Zheng L, Gan Y, Zhou M, Zhao K, Xu S, Wu B, Deng Z, Fu P. Amifostine ameliorates bleomycin-induced murine pulmonary fibrosis via NAD(+)SIRT1/AMPK pathway-mediated effects on mitochondrial function and cellular metabolism. *Eur J Med Res* 2024; **29**: 68 [PMID: 38245795 DOI: 10.1186/s40001-023-01623-4]
- 29** **Wei Z**, Jia J, Heng G, Xu H, Shan J, Wang G, Liu C, Xia J, Zhou H, Wu M, Yang Z, Wang M, Xiong Z, Huang H, Liu L, Qian C. Sirtuin-1/Mitochondrial Ribosomal Protein S5 Axis Enhances the Metabolic Flexibility of Liver Cancer Stem Cells. *Hepatology* 2019; **70**: 1197-1213 [PMID: 30901096 DOI: 10.1002/hep.30622]
- 30** **Vellinga TT**, Borovski T, de Boer VC, Fatrai S, van Schelven S, Trumpp K, Verheem A, Snoeren N, Emmink BL, Koster J, Rinkes IH, Kranenburg O. SIRT1/PGC1 α -Dependent Increase in Oxidative Phosphorylation Supports Chemotherapy Resistance of Colon Cancer. *Clin Cancer Res* 2015; **21**: 2870-2879 [PMID: 25779952 DOI: 10.1158/1078-0432.CCR-14-2290]
- 31** **Kato Y**, Maeda T, Suzuki A, Baba Y. Cancer metabolism: New insights into classic characteristics. *Jpn Dent Sci Rev* 2018; **54**: 8-21 [PMID: 29628997 DOI: 10.1016/j.jdsr.2017.08.003]
- 32** **Li YQ**, Sun FZ, Li CX, Mo HN, Zhou YT, Lv D, Zhai JT, Qian HL, Ma F. RARRES2 regulates lipid metabolic reprogramming to mediate the development of brain metastasis in triple negative breast cancer. *Mil Med Res* 2023; **10**: 34 [PMID: 37491281 DOI: 10.1186/s40779-023-00470-y]
- 33** **İlhan M**. Non-metabolic functions of pyruvate kinase M2: PKM2 in tumorigenesis and therapy resistance. *Neoplasma* 2022; **69**: 747-754 [PMID: 35471978 DOI: 10.4149/neo_2022_220119N77]
- 34** **Wong N**, Ojo D, Yan J, Tang D. PKM2 contributes to cancer metabolism. *Cancer Lett* 2015; **356**: 184-191 [PMID: 24508027 DOI: 10.1016/j.canlet.2014.01.031]
- 35** **Zhou Y**, Li F, Zou B, Zhou X, Luo L, Dong S, He Z, Zhang Z, Liao L, Liu H, Cai C, Gu D, Duan X. β -Arrestin2 promotes docetaxel resistance of castration-resistant prostate cancer via promoting hnRNP A1-mediated PKM2 alternative splicing. *Discov Oncol* 2023; **14**: 215 [PMID: 38019357 DOI: 10.1007/s12672-023-00740-0]
- 36** **Arifin WN**, Zahiruddin WM. Sample Size Calculation in Animal Studies Using Resource Equation Approach. *Malays J Med Sci* 2017; **24**: 101-105 [PMID: 29386977 DOI: 10.21315/mjms2017.24.5.11]
- 37** **Biller LH**, Schrag D. Diagnosis and Treatment of Metastatic Colorectal Cancer: A Review. *JAMA* 2021; **325**: 669-685 [PMID: 33591350 DOI: 10.1001/jama.2021.0106]
- 38** **Zimmermann M**, Li T, Semrad TJ, Wu CY, Yu A, Cimino G, Malfatti M, Haack K, Turteltaub KW, Pan CX, Cho M, Kim EJ, Henderson PT. Oxaliplatin-DNA Adducts as Predictive Biomarkers of FOLFOX Response in Colorectal Cancer: A Potential Treatment Optimization Strategy. *Mol Cancer Ther* 2020; **19**: 1070-1079 [PMID: 32029633 DOI: 10.1158/1535-7163.MCT-19-0133]
- 39** **Dienstmann R**, Salazar R, Tabernero J. Personalizing colon cancer adjuvant therapy: selecting optimal treatments for individual patients. *J Clin Oncol* 2015; **33**: 1787-1796 [PMID: 25918287 DOI: 10.1200/JCO.2014.60.0213]
- 40** **Argilés G**, Tabernero J, Labianca R, Hochhauser D, Salazar R, Iveson T, Laurent-Puig P, Quirke P, Yoshino T, Taieb J, Martinelli E, Arnold D; ESMO Guidelines Committee. Electronic address: clinicalguidelines@esmo.org. Localised colon cancer: ESMO Clinical Practice Guidelines for diagnosis, treatment and follow-up. *Ann Oncol* 2020; **31**: 1291-1305 [PMID: 32702383 DOI: 10.1016/j.annonc.2020.06.022]
- 41** **Su D**, Liu C, Cui J, Tang J, Ruan Y, Zhang Y. Advances and prospects of drug clinical research in colorectal cancer in 2022. *Cancer Innov* 2023; **2**: 99-113 [PMID: 38090057 DOI: 10.1002/cai2.62]
- 42** **Lee J**, Heo SC, Kim Y. Combination of oxaliplatin and β -carotene suppresses colorectal cancer by regulating cell cycle, apoptosis, and cancer stemness in vitro. *Nutr Res Pract* 2024; **18**: 62-77 [PMID: 38352212 DOI: 10.4162/nrp.2024.18.1.62]
- 43** **Zhou R**, Wen Z, Liao Y, Wu J, Xi S, Zeng D, Sun H, Wu J, Shi M, Bin J, Liao Y, Liao W. Evaluation of stromal cell infiltration in the tumor microenvironment enable prediction of treatment sensitivity and prognosis in colon cancer. *Comput Struct Biotechnol J* 2022; **20**: 2153-2168 [PMID: 35615026 DOI: 10.1016/j.csbj.2022.04.037]
- 44** **Ahluwalia P**, Ballur K, Leeman T, Vashishth A, Singh H, Omar N, Mondal AK, Vaibhav K, Baban B, Kolhe R. Incorporating Novel Technologies in Precision Oncology for Colorectal Cancer: Advancing Personalized Medicine. *Cancers (Basel)* 2024; **16**: 480 [PMID: 38339232 DOI: 10.3390/cancers16030480]
- 45** **Regan-Fendt K**, Li D, Reyes R, Yu L, Wani NA, Hu P, Jacob ST, Ghoshal K, Payne PRO, Motiwala T. Transcriptomics-Based Drug Repurposing Approach Identifies Novel Drugs against Sorafenib-Resistant Hepatocellular Carcinoma. *Cancers (Basel)* 2020; **12**: 2730 [PMID: 32977582 DOI: 10.3390/cancers12102730]
- 46** **Bhattacharya B**, Mohd Omar MF, Soong R. The Warburg effect and drug resistance. *Br J Pharmacol* 2016; **173**: 970-979 [PMID: 26750865 DOI: 10.1111/bph.13422]
- 47** **Feng J**, Zhang J, Chen Y. Prognostic value of a glycolysis and cholesterol synthesis related gene signature in osteosarcoma: implications for immune microenvironment and personalized treatment strategies. *Oncologie* 2024; **26**: 301-310 [DOI: 10.1515/oncologie-2023-0417]
- 48** **López-Lázaro M**. The warburg effect: why and how do cancer cells activate glycolysis in the presence of oxygen? *Anticancer Agents Med Chem* 2008; **8**: 305-312 [PMID: 18393789 DOI: 10.2174/187152008783961932]

- 49** **Graham NA**, Minasyan A, Lomova A, Cass A, Balanis NG, Friedman M, Chan S, Zhao S, Delgado A, Go J, Beck L, Hurtz C, Ng C, Qiao R, Ten Hoeve J, Palaskas N, Wu H, Müschen M, Multani AS, Port E, Larson SM, Schultz N, Braas D, Christofk HR, Mellinghoff IK, Graeber TG. Recurrent patterns of DNA copy number alterations in tumors reflect metabolic selection pressures. *Mol Syst Biol* 2017; **13**: 914 [PMID: 28202506 DOI: 10.1525/msb.20167159]
- 50** **Jin L**, Zhou Y. Crucial role of the pentose phosphate pathway in malignant tumors. *Oncol Lett* 2019; **17**: 4213-4221 [PMID: 30944616 DOI: 10.3892/ol.2019.10112]
- 51** **Pavlova NN**, Zhu J, Thompson CB. The hallmarks of cancer metabolism: Still emerging. *Cell Metab* 2022; **34**: 355-377 [PMID: 35123658 DOI: 10.1016/j.cmet.2022.01.007]
- 52** **Sever T**, Ellidokuz EB, Basbinar Y, Ellidokuz H, Yilmaz ÖH, Calibasi-Kocal G. Beta-Hydroxybutyrate Augments Oxaliplatin-Induced Cytotoxicity by Altering Energy Metabolism in Colorectal Cancer Organoids. *Cancers (Basel)* 2023; **15**: 5724 [PMID: 38136270 DOI: 10.3390/cancers15245724]
- 53** **Mou JJ**, Peng J, Shi YY, Li N, Wang Y, Ke Y, Zhou YF, Zhou FX. Mitochondrial DNA content reduction induces aerobic glycolysis and reversible resistance to drug-induced apoptosis in SW480 colorectal cancer cells. *Biomed Pharmacother* 2018; **103**: 729-737 [PMID: 29684851 DOI: 10.1016/j.biopharm.2018.04.099]
- 54** **Li Y**, Tang S, Shi X, Lv J, Wu X, Zhang Y, Wang H, He J, Zhu Y, Ju Y, Zhang Y, Guo S, Yang W, Yin H, Chen L, Gao D, Jin G. Metabolic classification suggests the GLUT1/ALDOB/G6PD axis as a therapeutic target in chemotherapy-resistant pancreatic cancer. *Cell Rep Med* 2023; **4**: 101162 [PMID: 37597521 DOI: 10.1016/j.xcrm.2023.101162]
- 55** **Chen T**, Xie S, Cheng J, Zhao Q, Wu H, Jiang P, Du W. AKT1 phosphorylation of cytoplasmic ME2 induces a metabolic switch to glycolysis for tumorigenesis. *Nat Commun* 2024; **15**: 686 [PMID: 38263319 DOI: 10.1038/s41467-024-44772-8]
- 56** **Shi T**, Ma Y, Cao L, Zhan S, Xu Y, Fu F, Liu C, Zhang G, Wang Z, Wang R, Lu H, Lu B, Chen W, Zhang X. B7-H3 promotes aerobic glycolysis and chemoresistance in colorectal cancer cells by regulating HK2. *Cell Death Dis* 2019; **10**: 308 [PMID: 30952834 DOI: 10.1038/s41419-019-1549-6]
- 57** **Zhao Z**, Wu MS, Zou C, Tang Q, Lu J, Liu D, Wu Y, Yin J, Xie X, Shen J, Kang T, Wang J. Downregulation of MCT1 inhibits tumor growth, metastasis and enhances chemotherapeutic efficacy in osteosarcoma through regulation of the NF-κB pathway. *Cancer Lett* 2014; **342**: 150-158 [PMID: 24012639 DOI: 10.1016/j.canlet.2013.08.042]
- 58** **Rajamohan SB**, Pillai VB, Gupta M, Sundaresan NR, Birukov KG, Samant S, Hottiger MO, Gupta MP. SIRT1 promotes cell survival under stress by deacetylation-dependent deactivation of poly(ADP-ribose) polymerase 1. *Mol Cell Biol* 2009; **29**: 4116-4129 [PMID: 19470756 DOI: 10.1128/MCB.00121-09]
- 59** **Patra S**, Praharaj PP, Singh A, Bhutia SK. Targeting SIRT1-regulated autophagic cell death as a novel therapeutic avenue for cancer prevention. *Drug Discov Today* 2023; **28**: 103692 [PMID: 37379905 DOI: 10.1016/j.drudis.2023.103692]
- 60** **Chen F**, Kolben T, Meister S, Czogalla B, Kolben TM, Hester A, Burges A, Trillsch F, Schmoekel E, Mayr D, Mayerhofer A, Mahner S, Jeschke U, Beyer S. The role of resveratrol, Sirtuin1 and RXR α as prognostic markers in ovarian cancer. *Arch Gynecol Obstet* 2022; **305**: 1559-1572 [PMID: 34870752 DOI: 10.1007/s00404-021-06262-w]
- 61** **Yin X**, Liu Z, Wang J. Tetrahydropalmatine ameliorates hepatic steatosis in nonalcoholic fatty liver disease by switching lipid metabolism via AMPK-SREBP-1c-Sirt1 signalling axis. *Phytomedicine* 2023; **119**: 155005 [PMID: 37562090 DOI: 10.1016/j.phymed.2023.155005]
- 62** **Dizdar O**, Arslan C, Altundag K. Advances in PARP inhibitors for the treatment of breast cancer. *Expert Opin Pharmacother* 2015; **16**: 2751-2758 [PMID: 26485111 DOI: 10.1517/14656566.2015.1100168]
- 63** **Muñoz-Gámez JA**, Martín-Oliva D, Aguilera-Quesada R, Cañuelo A, Nuñez MI, Valenzuela MT, Ruiz de Almodóvar JM, De Murcia G, Oliver FJ. PARP inhibition sensitizes p53-deficient breast cancer cells to doxorubicin-induced apoptosis. *Biochem J* 2005; **386**: 119-125 [PMID: 15456408 DOI: 10.1042/BJ20040776]



Published by **Baishideng Publishing Group Inc**
7041 Koll Center Parkway, Suite 160, Pleasanton, CA 94566, USA
Telephone: +1-925-3991568
E-mail: office@baishideng.com
Help Desk: <https://www.f6publishing.com/helpdesk>
<https://www.wjnet.com>

